Research Article

Development of an accurate "composition-process-properties" dataset for SLMed Al-Si-(Mg) alloys and its application in alloy design

Tianchuang Gao[1], Jianbao Gao[1,*] iD, Jinliang Zhang[2], Bo Song[2], Lijun Zhang[1,*] iD

[1]State Key Laboratory of Powder Metallurgy, Central South University, Changsha 410083, Hunan, China.
[2]State Key Laboratory of Materials Processing and Die & Mould Technology, Huazhong University of Science and Technology, Wuhan 430074, Hubei, China.

*Correspondence to:** Dr. Jianbao Gao, State Key Laboratory of Powder Metallurgy, Central South University, Lushannan Road No. 932, Changsha 410083, Hunan, China. E-mail: jianbao.gao@csu.edu.cn; Prof. Lijun Zhang, State Key Laboratory of Powder Metallurgy, Central South University, Lushannan Road No. 932, Changsha 410083, Hunan, China. E-mail: lijun.zhang@csu.edu.cn

Abstract

Al-Si-Mg series alloys are the most common alloys available for additive manufacturing forming with low cracking tendency. However, there is no systematic study on the computational design of SLMed Al-Si-(Mg) alloys due to the huge parameter space of composition and processes. In this paper, a high-quality dataset of SLMed Al-Si-(Mg) alloys containing 176 pieces of data from 50 publications was first established, which recorded the information, including alloy compositions, process parameters, test conditions, and mechanical properties. A threshold value of 35 J/mm^3 for energy density (Ed) was then proposed as a criterion to clean the data points with lower ultimate tensile strength (UTS) and elongation (EL). The cleaned dataset consists of a first training/testing dataset with 142 data for model construction and a second testing dataset with 9 data for model verification. After that, four machine learning models were applied to establish the quantitative relation of "composition-processes-properties" in SLMed Al-Si-(Mg) alloys. The MLPReg model was chosen as the optimal one considering its best performance and subsequently utilized to design novel compositions and process parameters for SLMed Al-Si-(Mg) alloys. The UTS and EL of the designed alloy with a maximum comprehensive mechanical property are 549 MPa and 16%, both of which are higher than all the available experimental data. It is anticipated that the present design strategy based on the machine learning method should generally be applicable to other SLMed alloy systems.

INTRODUCTION

Due to their low density, high specific strength, high specific stiffness, and good plasticity, aluminum alloys are the preferred lightweight structure materials in aerospace, automotive, ships, and other fields[1]. The rapid development of marine, aerospace, and automotive transportation has put forward strict requirements for the performance of alloys. Selective laser melting (SLM) forming technology, as a promising additive manufacturing (AM) technology[2], has the advantages of a fast cooling rate and grain refinement. It can improve the mechanical properties of alloys and prepare parts with complex shapes, which greatly broadens the application range of aluminum alloys. Among different types of aluminum alloys, the Al-Si-(Mg) (i.e., Al-Si and Al-Si-Mg) series alloys are one of the few aluminum alloy systems suitable for the additive manufacturing process, including Al4Si[3,4], Al12Si[5-7], AlSi10Mg[8-10], and AlSi7Mg[11,12], etc. In particular, alloys with near-eutectic compositions over a very narrow solidification temperature range of 40K~50K can greatly reduce the risk of cracking during the laser additive manufacturing process and enable the preparation of nearly fully dense products, thus receiving extensive research attention.

The mechanical properties of SLMed Al-Si-(Mg) alloys are closely related to their composition and complex processing parameters. For instance, 0.2~0.4 wt.% Mg content may enhance the strength of alloys through precipitation hardening due to the precipitation of the fine Mg_2Si phase during the aging heat treatment or the AM process[9,11,13]. Furthermore, the specific process parameters of the SLM process significantly affect the alloy properties, including laser power[14-16], scanning speed[16,17], powder layer thickness[15], scanning spacing[18,19], build direction[20-22], scanning strategy[23,24], and post heat-treatment processes[13,11,20]. Though a number of experimental investigations have been devoted to different SLMed Al-Si-(Mg) alloys in the literature, the factors that affect the properties and performance of alloys are too many, and thus there is still no systematic study on the relation among the "composition-process-properties" of the SLMed Al-Si-(Mg) alloys. Thus, there is an urgent need to solve this problem because it may block the efficient design of high-performance SLMed Al-Si-(Mg) alloys over high-dimensional parameter space.

To solve this problem, a variety of computational methods at different scales, including CALculation of PHAse Diagram (CALPHAD)[25-30], phase-field modeling[31-33], finite element simulation[34], and machine learning (ML)[28,29,35,36] can be utilized. Among them, ML is one of the most efficient computational methods. It can be utilized to establish the quantitative relation of "composition-processes-properties", and even accelerate the design of high-performance alloys over a high dimensional parameter space. Mondal *et al.*[37] employed a physical information-based machine learning method to systematically investigate the cracking mechanism of SLMed 6061Al, 2024Al, and AlSi10Mg alloys. The decision trees, support vector machines, and logistic regression techniques were used to predict crack formation conditions, and the cracking susceptibility maps were established for optimizing the process parameters. Yu *et al.*[38] used AdaBoost, gradient tree boosting, K-nearest neighbors, decision tree, and Extra Trees regressors to successfully predict the hardness and relative mass density of LPBFed CNTs/AlSi10Mg nanocomposites with cellular structure features as input. The relative errors of the predicted hardness and relative mass density due to the optimal model are as low as 3.61% and 1.42%, respectively. He *et al.*[39] applied a gaussian process regression-based machine learning approach to establish a processing window for a high-density additive manufactured 2-vol% TiCN reinforced AlSi10Mg composite. Though the ML approach has been widely used to design process parameters for SLMed Al alloys, there is still a lack of reports on the establishment of a high-quality "composition-process-properties" dataset of the basic SLMed Al-Si-(Mg) alloys using the ML approach. Such a situation urgently needs to be improved.

Consequently, based on the ML approach together with an exhausting collection of literature data, an accurate "composition-process-properties" dataset for the basic but technically important SLMed Al-Si-(Mg) alloys is to be developed, and then applied to design the SLMed Al-Si-(Mg) alloys with better mechanical properties than the literature reports. In the next section, a brief introduction to the ML approach is given, followed by the data collection and pre-processing of the dataset, including the data cleaning and feature analysis. After that, four ML models are employed to establish the quantitative relation of "composition-processes-properties" in the SLMed Al-Si-(Mg) alloys, and the optimal one for best reproducing the training and testing sets is to be selected. The selected ML model is subsequently applied to discover the novel compositions and processing parameters of as-built Al-Si-(Mg) alloys with better mechanical properties than the literature reports. Finally, a conclusion of this paper is drawn.

MACHINE LEARNING APPROACH

The machine learning approach can establish an intrinsic relation between the input and output layers by systematically analyzing each characteristic variable in the data, thus realizing the prediction of new data. The basic ML workflow in alloy design mainly includes data collection, data cleaning, feature analysis, model selection, model training, model verification, and prediction analysis. In this paper, four machine learning models were built and comprehensively compared with each other to select the one with the highest accuracy, including linear regression (LinearReg), multi-layer perceptron regression (MLPReg), random forest regression (RFReg), and k-nearest neighbors (K-NN) regression.

LinearReg is widely utilized to construct a linear relationship between the target values and the characteristic variables by adjusting the regression coefficients. MLPReg is an artificial neural network that has a single input layer, one or more hidden layers, and a single output layer of perceptron, which is constituted by numerous neurons. The quantified relation between target values and variables is obtained by different weights and deviations in each neuron. The RFReg model consists of multiple mutually unrelated decision trees, each of which yields a prediction result from randomly selected samples and features, and the prediction result is obtained by combining the results of all trees and taking the average. The model has the function of calculating the importance of features. When the K-NN regressor is used for prediction, the mean value of the nearest data point is chosen as the prediction value.

In order to avoid the order of magnitude difference between each dimension of the dataset, resulting in inaccurate prediction results, all the variables need to be standardized before constructing the model. The data then obey a normal distribution with a mean of 0 and a variance of 1 (i.e., standard normal distribution). The equation of standardization treatment is given as

$$Z = (X - \mu)/\sigma \tag{1}$$

where Z is the return value, μ is the mean of the training samples, and σ is the standard deviation of the training samples.

Two metrics methods were utilized to evaluate the quality of machine learning models, i.e., the mean absolute error (MAE) and the coefficient of determination (R^2). The MAE measures the relative magnitude of deviation, while the R^2 can be used to characterize the fitness level of the model. They are respectively defined as

$$MAE\ (y, y') = \frac{1}{n} \sum_{i=1}^{n} (y_i - y_i')^2 \qquad (2)$$

$$R^2(y, y') = 1 - \frac{\sum_{i=1}^{n}(y_i - y_i')^2}{\sum_{i=1}^{n}(y_i - \bar{y})^2} \qquad (3)$$

In Equations (2) and (3), y_i' is the prediction value of the ith data, y_i is the actual value corresponding to it, while n is the size of the dataset.

DATA COLLECTION AND PRE-PROCESSING

Data collection

The mechanical properties [including ultimate tensile strength (UTS), yield strength (YS), and elongation (EL)] of the SLMed alloys do not only depend on the compositions[40-47] and processes[48-54] but also the testing condition[55-59]. Therefore, in order to study the influencing factors affecting the mechanical properties of SLMed Al-Si-(Mg) alloy, the compositions[60-62] (i.e., Si and Mg contents), the manufacturing processes (including laser power[63-65], scanning speed[66,67], scanning spacing[68-70], powder layer thickness[71,72], hatching space[73], and rotation angle[74]), and the testing direction[75,76] should be considered at the same time. However, it is quite challenging to analyze data in high-dimensional characteristic variable space, and the dimension of the characteristic variable thus needs to be reduced. The energy density (Ed)[77-79] is commonly used to describe the combined effect of laser power, scanning speed, scanning spacing, powder layer thickness, and hatching space on alloy properties. Ed can be calculated by using the following equation,

$$Ed = P/(v \times h \times t) \qquad (4)$$

where P is laser powder, v is scan speed, h is hatch space, and t is layer thickness. Besides, the testing direction and the rotation angle should also be considered during data analysis. The testing direction describes the test situation. The tensile direction is regarded as 0° when it is parallel to the substrate plane, while 90° when it is vertical to the substrate plane. Moreover, the rotation angle represents the successive layer rotation during the additive manufacturing process.

In order to make the dataset more reliable and accurate, the following guidelines were obeyed during the data collection:

(*i*) Only the data of Al-Si-(Mg) alloys manufactured by SLM techniques were collected;

(*ii*) The data reported in the literature must be complete, and all the information on the composition, process parameters, and mechanical properties should be included;

(*iii*) If no actual alloy composition was given in the literature, the nominal composition of the alloy was used instead.

The data sets of as-built SLMed Al-Si-(Mg) alloys, which include 176 pieces of data from 50 publications, were established in the present work and displayed in the Supplementary Materials. Figure 1A and B shows the distribution of UTS, YS, and EL for different SLMed Al-Si-(Mg) alloys, mainly including Al4Si[3,4], Al7SiMg[12,13,24,49-60], AlSi10Mg[9-11,61-79], and Al12Si[4,5,14,40-48]. It is clearly observed in the figure that the strength
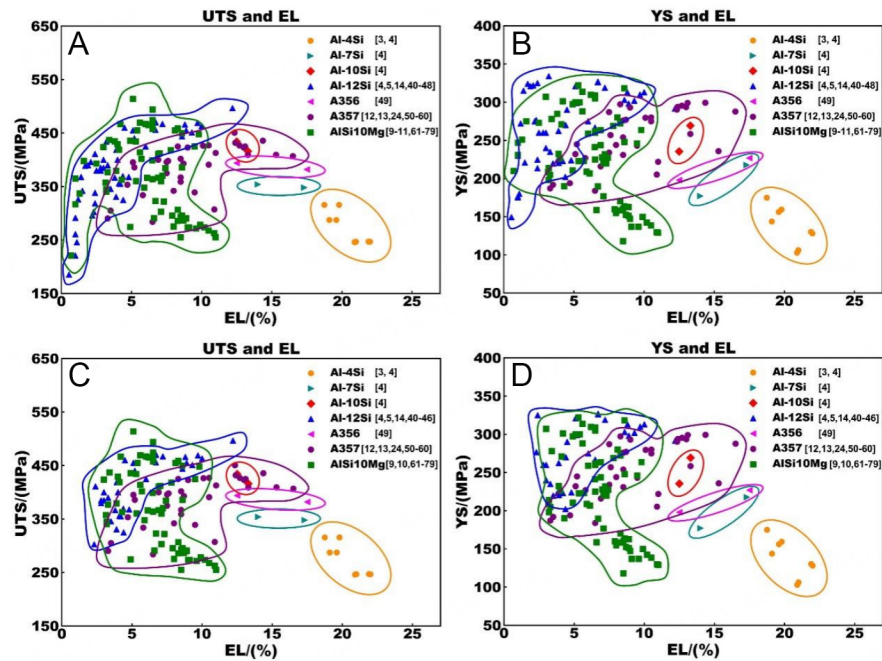
Figure 1. Distribution of UTS~EL and YS~EL data in different SLMed Al-Si-(Mg) alloys including Al4Si, Al7Si, Al10Si, Al12Si, A356, A357, and AlSi10Mg: (A) and (B) raw data; (C) and (D) data with cleaning. EL: elongation; UTS: ultimate tensile strength; YS: yield strength.

of the alloys tends to increase as the Si content increases while the elongation of the alloys decreases. The maximum UTS value is 514MPa from the AlSi10Mg (wt.%) alloy[77], while the maximum EL value is 22% from the Al4Si (wt.%) alloy[4]. However, there is a region with both poor strength and elongation, which is the lower left corner in Figure 1A. The detailed statistical results of all data are shown in Supplementary Table 1. It shows the statistical results of the composition of each element, Ed, rotation angle, tensile direction, UTS, YS, and EL among the 176 data. The range of Ed is from 13.33 J/mm^3 to 176.19 J/mm^3. The rotation angle mainly includes 45°, 67°, 73°, and 90°.

Data cleaning

In order to precisely design alloys with excellent performance, the data with relatively high mechanical properties need to be retained as much as possible while avoiding the impact of low-performance data. Before constructing the model, a data cleaning by abandoning the data with lower mechanical properties is thus needed. The cleaned datasets are detailly shown in Figure 1C and D and Supplementary Table 2 and are to be used for constructing and validating the ML model. As shown in Figure 1C and D, the data for Al12Si and AlSi10Mg alloys with both poor strength and ductility were cleaned according to their lower Ed (≤ 35 J/mm^3). Finally, the cleaned dataset includes a first training/testing dataset with 142 data for model construction and a second testing dataset with 9 data for model verification.

To investigate the key factors affecting the mechanical properties of the SLMed Al-Si-(Mg) alloys, three main characteristic variables (i.e., Ed, layer rotation, and test direction) and their effect on the properties in three representative Al-Si-(Mg) alloys (i.e., Al12Si, AlSi10Mg, and Al7SiMg) were systematically analyzed. As shown in Figure 2A and B, the Ed is one of the most critical parameters in the fabrication process and also plays a key role in mechanical properties. The results indicate that the alloy with lower Si content requires higher Ed, which may be caused by the lower energy absorption of Al. Interestingly, there are also some very limited cases for the AlSi10Mg alloy with higher UTS and EL fabricated by high Ed (≥ 130 J/mm^3), which needs further consideration and verification. For the Al12Si and AlSi10Mg alloys, most of them tend
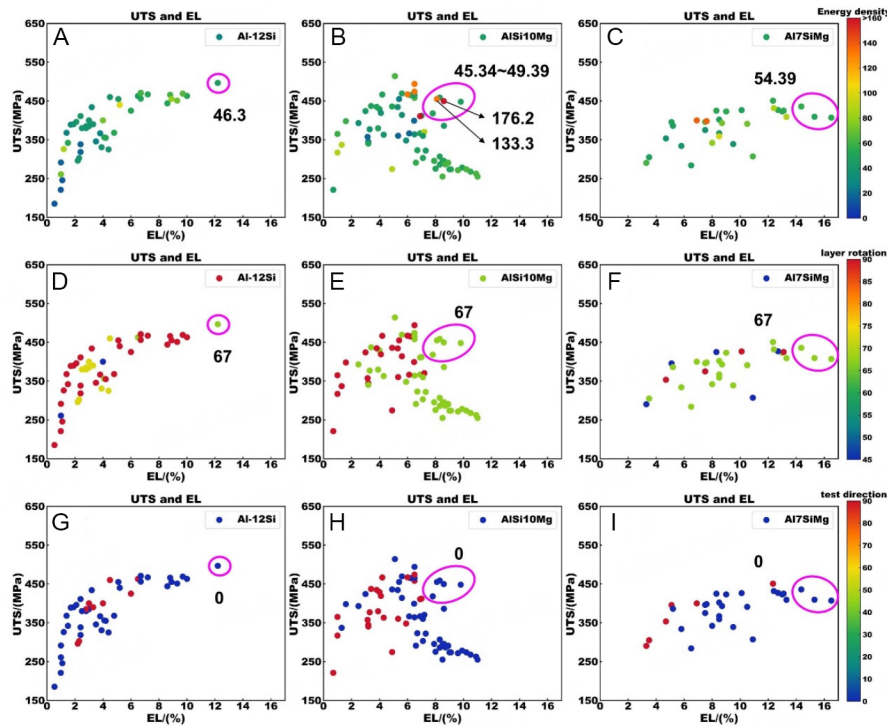
Figure 2. Effect of different characteristic variables (i.e., Ed, layer rotation, and test direction) on the mechanical properties of different SLMed Al-Si-(Mg) alloys: (A), (D), and (G) Al12Si alloys; (B), (E), and (H) AlSi10Mg alloys; (C), (F), (I) Al7SiMg alloys. Ed: energy density; EL: elongation; UTS: ultimate tensile strength.

to behave with low tensile strength and weak ductility when the Ed is low (≤ 30~40 J/mm³). Therefore, in order to design high-performance alloys, some data points with Ed lower than 35 J/mm³, especially for Al12Si alloy in the lower left region, should be deleted during the data cleaning.

Figure 2D-F and Figure 2G-I show the effect of rotation angle and testing direction on the properties. The results demonstrate that the UTS and EL of the alloys are much lower when both the rotation angle and the testing direction are 90°. Moreover, all the high-performance data points occur with a combination of layer rotation of 67° and test direction of 0°. This fact may be associated with the grain size and combination of neighboring powder layers during the additive manufacturing process[23]. With an optimal layer rotation, the fully densified parts with refined grain size can be fabricated. Meanwhile, directional solidification in SLM leads to preferential grain growth along the <100> direction, and the resulting intense texture is the main reason for the anisotropy of the alloy[80]. Thijs *et al.*[80] found a strong <100> texture along the scanning direction (i.e., parallel to the substrate plane) in SLMed AlSi10Mg alloy. It led to higher UTS and EL in alloys along the 0° test direction. However, an interesting observation was also found in some literature reports[12,49,53,54,56,66,68-70,72,74,75], as shown in Supplementary Figure 1. Under the same preparation conditions, the alloys with a test direction of 90° can also exhibit higher UTS. Kimura *et al.*[49] found the presence of coarsened microstructure encompassing the borders of laser scan tracks, which led to a lower UTS for horizontal alloys. Meanwhile, Kumar *et al.*[81] discovered that the distribution of molten particles along the vertical direction has a strong inter-particle bond, which plays a role in enhancing the strength of the alloy, but also increases the brittle behavior. As a result, they show a higher UTS but with a lower EL compared with the other alloys. Hence, in the Al-Si-(Mg) alloys, the influence of different features on the alloy properties is complex, and it is difficult to obtain the ideal target alloy by simple data analysis or limited experiments.

Some data points with good performance in three alloy systems were selected and analyzed, as marked by the purple circles in Figure 2. In general, from the current dataset, the promising Ed for Al-Si-(Mg) alloy is roughly distributed between 45 J/mm^3 and 55 J/mm^3. As the Si content increases, the suitable Ed value decreases. It seems that the combination of 67° layer rotation and 0° test direction provide great opportunities to obtain high-performance alloy. Based on the existing experimental dataset, the effect of more manufacturing parameters (laser power, scan speed, hatch space, and layer thickness) on the mechanical properties of SLMed Al-Si-(Mg) alloys were further investigated and analyzed, as shown in Supplementary Figure 2. The suitable layer thickness is 30 μm~40 μm, while the suitable hatch space is 100 μm~130 μm. With the Si content decreasing, the suitable laser power varies from 250 W to 370 W, while the suitable scan speed can vary from 1,800 mm/s to 1,300 mm/s.

Feature analysis

After the data cleaning, the correlations between the characteristic variables and the mechanical properties were analyzed. As shown in Figure 3, Pearson's correlation coefficient for the characteristic and alloy properties was calculated. The results show that the correlation coefficient between any two variables is totally lower than 0.8, except for UTS and YS. The correlation coefficients between UTS and YS are as high as 0.92, with a strong linear relationship. Thus, the strength of the alloy can be described by using only UTS. Moreover, the correlation coefficients between the input variables (i.e., W(Si) and W(Mg), Ed, layer rotation, and test direction) and mechanical properties (i.e., UTS, YS, and EL) are very low. It means that there is no strong linear relationship between any two of them, and the alloy properties are not obtained by a simple linear summation of each variable's contribution. Therefore, the machine learning model (either MLPReg model or RFReg model), which can describe the complex unknown relationship for multi-variables, should be used to construct the relation of "composition-process-properties" in SLMed Al-Si-(Mg) alloys.

RESULTS AND DISCUSSION
Model construction and selection

Based on the constructed data set, the next key is to establish a quantitative relationship among alloy compositions, manufacturing parameters, and mechanical properties by machine learning technique. Five feature variables (W(Si), W(Mg), Ed, layer rotation, and test direction) were used as the input layer to predict UTS, YS, and EL simultaneously.

In order to select the most suitable model, four machine learning models were used to establish the quantitative relationship, including LinearReg, MLPReg, RFReg, and K-NN regressor. The randomized search strategy combining 5-fold cross-validation was utilized to find the optimal hyperparameters, based on which the optimal combinations of model parameters were selected. All the data were randomly divided into training and test sets with a 9:1 ratio.

Figure 4 presents the MAE value and R^2 score of the above four models based on the cleaned dataset. The lower MAE and the larger the R^2 score, the better the predictive performance. As shown in Figure 5, the LinearReg presents the poorest performance with R^2 less than 0.5 and MAE higher than 30. For the K-NN model with the lowest MAE value, it may be overfitting because the R^2 deviation between the testing set and the training set is large while the R^2 score of the training set is approaching 1. Both MLPReg and RFReg have good performance in training and testing sets; the R^2 score of the training set for these two models are 0.8962, 0.8216, and 0.8985, 0.8452 for the testing set, respectively. To further investigate the accuracy and stability of the model, the size of the testing set changed from 10% to 40%, and the evolution of the R^2 score was recorded in Supplementary Figure 3. The results also show that the testing set R^2 score of K-NN
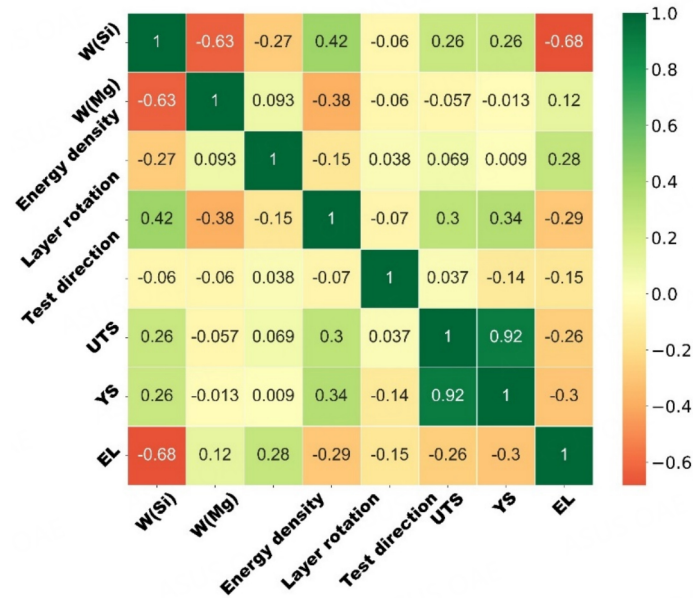
Figure 3. Pearson's correlation coefficients between characteristic variables and alloy properties. EL: elongation; UTS: ultimate tensile strength; YS: yield strength.
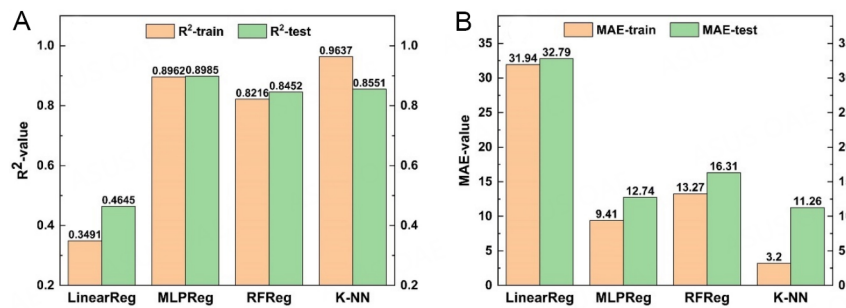
Figure 4. (A) R^2 score and (B) MAE value of different models on 90% training set and 10% testing set. MAE: mean absolute error.
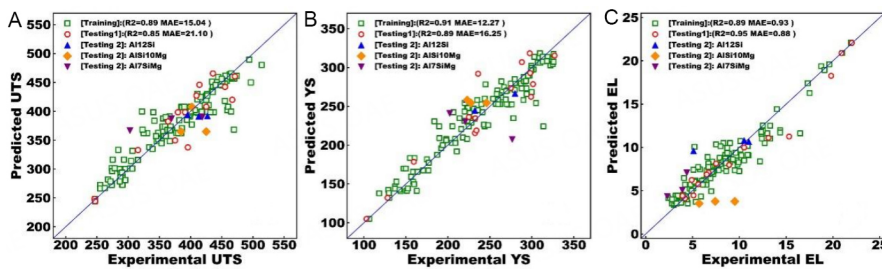
Figure 5. Performance of the MLPReg model predicted (A)UTS; (B)YS; and (C)EL on the training set and the testing set. EL: elongation; UTS: ultimate tensile strength; YS: yield strength.

dropped dramatically with the increased size due to the overfitting. Moreover, compared with the RFReg model, the MLPReg has a higher score overall. Therefore, the MLPReg model was selected as the optimal model to construct the quantitative relation of "composition-process-properties" in SLMed Al-Si-(Mg) alloy.

Validation and prediction for the selected ML model

Based on the selected MLPReg model, the model hyperparameters were optimized by a random search strategy with a 10% testing dataset. The structure of the optimized MLPReg model was 5 × 100 × 200 × 3 (1 input layer with 5 features, 2 hidden layers with 100 and 200 neurons, and 1 output layer with 3 output features). The detailed optimization results are displayed in Supplementary Table 3. The comparison between the predicted and experimental properties of the trained MLPReg model is shown in Figure 5. When the predicted result is very close to the actual value, the data point should be in the vicinity of the line $y = x$. The results show that the predicted UTS, YS, and EL are in good agreement with the experimental results on both the training and testing set. The average R^2 score of training and testing sets can reach 0.8962 and 0.8985.

Besides, different operators and experimental environments can affect the mechanical properties of the target alloy. In order to test the generality of the model and further verify the model accuracy, 3 representative alloys were selected from each of the three systems[5,48,58,59,78,79] (i.e., Al7SiMg, AlSi10Mg, Al12Si) from the cleaned dataset as the second test set. The composition and manufacturing parameters of those 9 alloys are shown in Supplementary Table 4. The comparison of predicted and experimental results of the second test set is also shown in Figure 5. The results showed that the selected ML model can predict the UTS, YS, and EL of all the alloys simultaneously, especially reproducing the mechanical properties of the 9 alloys in the second test dataset well. Therefore, it indicates that the presently selected ML model can simultaneously predict the UTS, YS, and EL of all the SLMed Al-Si-(Mg) alloy with high accuracy and will be utilized to design the alloy with high performance further.

Based on the trained and validated MLPReg model, the mechanical properties of alloys over a wide range of composition and process parameters can be predicted. A method for randomly generating composition and processes over the parameter space was used to create the big input dataset in this work. The range of Si is between 4.1wt.% and 12.1wt.% with $\Delta w(Si)$ = 1wt.%, and that of Mg varies from 0wt.% to 0.6wt.% with $\Delta w(Mg)$ = 0.1wt.%. The value of Ed varies from 26 J/mm^3 to 171 J/mm^3 with a step of 5 J/mm^3. Supplementary Table 2 shows that over 95% of the high-performance alloys were prepared using 67°, 73°, or 90° as the layer rotation angle. To achieve the best performance and increase the computational efficiency, three values (i.e., 67°, 73°, and 90°) were selected as candidates to make predictions. Figure 6 shows the predicted results based on the trained MLPReg model for random 11,300 data (combinations of compositions and processes) in SLMed Al-Si-(Mg) alloy. The plot has been colored with Quality Index (QI). The strength-ductility trade-off relationship indicates that monolithic materials have a limitation in achieving simultaneously high strength and elongation. In Figure 6, the alloys with high performance (i.e., high QI) usually presented a high strength with medium elongation.

To further validate the accuracy of the model, the predicted data with 7 wt.%, 10 wt.%, and 12 wt.% Si were extracted respectively and compared with the experimental results, as shown in Figure 7. The results indicated that all the experimental data locates in the region of the predicted results, inferring that the model can not only describe the properties of the existing experimental data very well but also predict the mechanical properties of the alloys over the unknown region(s).

Alloy design with desired mechanical properties

Based on the accurate prediction results over wide composition and process parameter space, one can design the SLMed Al-Si-(Mg) alloy with desired machinal properties. However, how to design an alloy with simultaneously high strength and ductility needs to be considered. The multi-objective to single-objective optimization strategy, which converts a weighted linear combination of multi-objective performance into a single objective for optimizing the design for a single objective quantity (Ashby's method[82]), is one of the
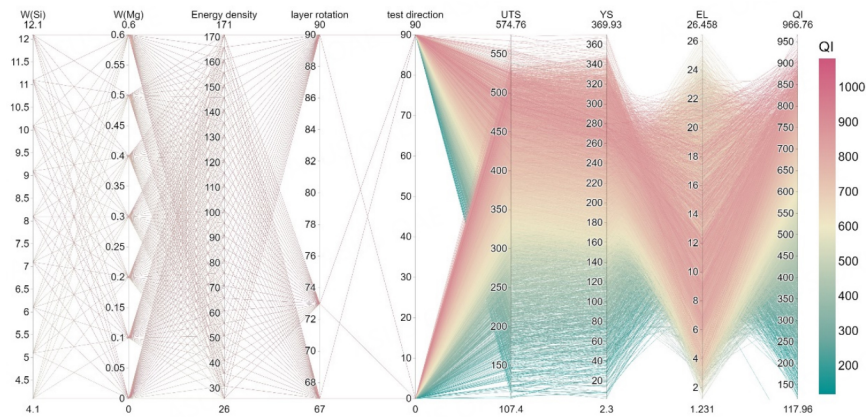
Figure 6. Results from MLPReg model prediction displayed as a parallel coordinate plot for 11300 combinations of compositions and process of Al-Si-(Mg) alloy. The plot is colored with Quality Index (QI). EL: elongation; UTS: ultimate tensile strength; YS: yield strength.
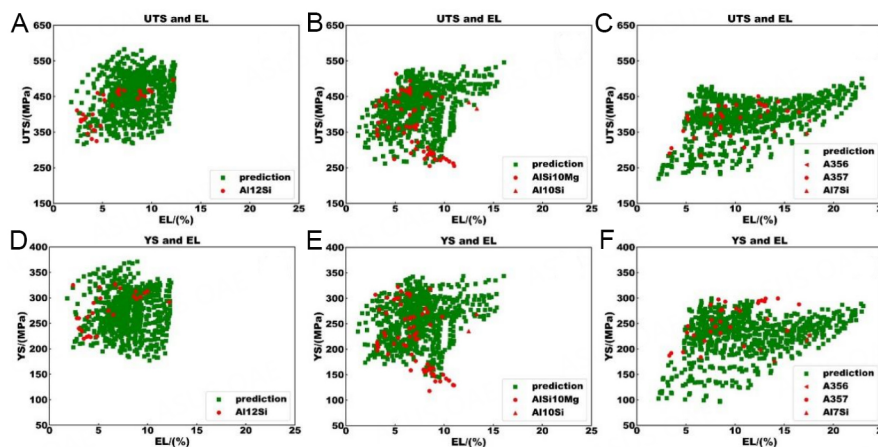
Figure 7. Distribution of predicted and experimental data (i.e., UTS, YS, and EL) in alloys with different Si contents: (A) and (D)12 wt.%; (B) and (E) 10 wt.%; (C) and (F) 7 wt.%. EL: elongation; UTS: ultimate tensile strength; YS: yield strength.

commonly used multi-objective optimization strategies and thus utilized in this work. The QI, which represents the evaluation criterion for alloy properties considering both strength and ductility, was employed in this work to design the alloy with optimal comprehensive mechanical properties. QI can be calculated by the following formula,

$$QI = UTS + YS \times log_{10}(EL) \qquad (5)$$

While the machine learning model, which can accurately predict the mechanical properties of the SLMed Al-Si-(Mg) alloys, has been established in this work, the QI can be used to find novel SLMed Al-Si-(Mg) alloys with higher comprehensive mechanical properties than all the experimental data reported in the literature based on the trained MLPReg model.

In order to make the recommended alloys as reasonable as possible, the contents of alloying elements and manufacturing parameter values of all the recommended alloys should not exceed the range of the training data set. According to the above discussion, the Ed of 35 J/mm³ is the threshold value for good mechanical

Table 1. Presently designed alloys with respective maximum UTS, maximum YS, maximum EL, and maximum QI under as-build conditions

Group	W(Si) (wt%)	W(Mg) (wt%)	Ed (J/mm³)	Rotation (°)	Direction (°)	UTS (MPa)	YS (MPa)	EL (%)	QI (MPa)
1	12.1	0.6	36	67	90	559.0	344.8	6.2	831.5
2	12.1	0.6	36	73	0	548.9	362.8	7.4	863.7
3	4.1	0	96	90	0	307.4	162.9	24.5	533.8
4	10.1	0.1	66	90	0	549.4	346.1	16.1	966.8
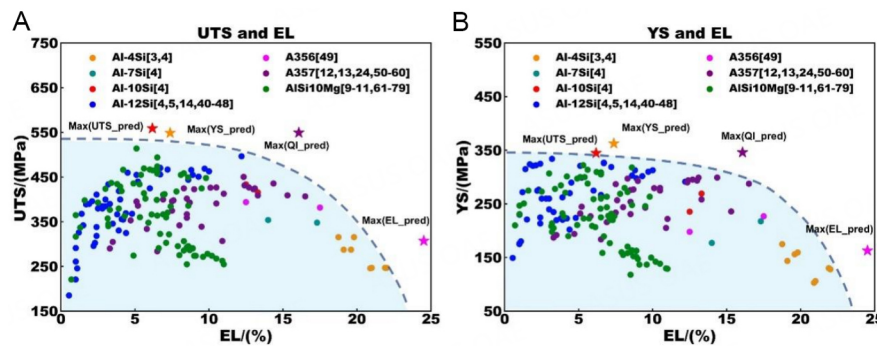
Figure 8. Presently designed alloys with respective maximum UTS, YS, EL, and QI, compared with as-built experiment data in different plots: (A) UTS-EL; (B)YS-EL. EL: elongation; QI: Quality Index; UTS: ultimate tensile strength; YS: yield strength.

properties. The analysis of the dataset in Supplementary Table 2 shows that 75% of the data points have an Ed below 62 J/mm³, with only a few special points larger than 100 J/mm³. Therefore, the alloys with Ed lower than 35 J/mm³ (threshold value) and higher than 100 J/mm³ (extreme value) were excluded here.

After predictions with random combinations of compositions and processes, the selected alloys with maximum UTS, maximum YS, maximum EL, or maximum QI are listed in Table 1. It can be clearly seen from the predicted results that the alloy with higher Si content owns higher strength. On the contrary, the highest elongation is achieved when the Si content is only 4%. The high-performance alloy with maximum QI can be obtained when the Si content is 10%. Such phenomena are consistent with the previously known experimental results[11,57,83], which further reinforces the reliability of the dataset and the accuracy of the model. This fact also indicates that the model not only deepens our understanding of the SLMed Al-Si-(Mg) system but also helps us to design new alloys.

The comparison between the design results and the original experimental dataset is shown in Figure 8. In the cleaned experimental datasets, the maximum value of UTS is 514 MPa. While in the predicted dataset based on the trained MLPReg model, the UTS of alloys can reach 560 MPa with the EL higher than 6%. The test direction for this alloy is 90°, which is consistent with some literature[12,68,70] and the data analysis above. This also indicates that the predicted results are reasonable. Moreover, for the designed alloy with a maximum QI of 966 MPa, its UTS is 549 MPa, and EL is 16%, both of which are higher than all the available experimental data. Although the designed results generally conform to the current experimental rules, their accuracy still needs further experimental validation as the major target for the next publication.

CONCLUSIONS

● Based on an exhausting collection from 50 publications, a high-quality dataset for SLMed Al-Si-(Mg) alloys (including Al12Si, Al10Si, AlSi10Mg, Al7Si, Al7SiMg, and Al4Si) with 176 pieces of data was

established. The dataset records the information on alloy composition, process parameters, test conditions, and mechanical properties in detail. The effect of three main variables (i.e., Ed, layer rotation, and test direction) on the mechanical properties was systematically analyzed in the three representative alloys (Al12Si, AlSi10Mg, and Al7SiMg). A threshold value of 35 J/mm^3 for Ed was used as a criterion to clean the data points with lower UTS and EL. The cleaned dataset consists of a first training/testing dataset with 142 data for model construction and a second testing dataset with 9 data for model verification.

● Four ML models were employed to establish the quantitative relation of "composition-processes-properties" in SLMed Al-Si-(Mg) alloys. After a comprehensive comparison, the MLPReg model was selected due to its best performance on both training and testing sets. The selected MLPReg model was then utilized to design novel compositions and process parameters for SLMed Al-Si-(Mg) alloys with maximum UTS, YS, EL, and comprehensive mechanical property index QI. For the alloy with maximum QI, its UTS can reach 549.4MPa, which is ~40MPa higher than the best one over the available experimental data, while its elongation can still retain 16%.

● The successful demonstration in this paper indicates that the present design strategy driven by the ML technique should generally be applicable to other SLMed alloy systems.

DECLARATIONS
Authors' contributions
Establishment, selection, and verification of machine learning model: Gao T
Made contributions to the conception and design of the study: Gao T, Gao J, Zhang L
Literatures data collation, interpretation, analysis, cleaning, and construction of data set, drafted the manuscript: Gao T, Gao J, Zhang J
Supervised, revised, and finalized the manuscript: Gao T, Gao J, Zhang J, Song B, Zhang L

Availability of data and materials
The using data set and the trained machine learning model can be seen in Supplementary Materials.

Financial support and sponsorship

Conflicts of interest
All authors declared that there are no conflicts of interest.

Ethical approval and consent to participate
Not applicable.

Consent for publication
Not applicable.

Copyright

REFERENCES

1. Zhang J, Song B, Wei Q, Bourell D, Shi Y. A review of selective laser melting of aluminum alloys: Processing, microstructure, property and developing trends. *J Mater Sci Technol* 2019;35:270-84. DOI

2. Ghio E, Cerri E. Additive manufacturing of AlSi10Mg and Ti₆Al₄V lightweight alloys via laser powder bed fusion: a review of heat treatments effects. *Materials* 2022;15:2047. DOI PubMed PMC

3. Kimura T, Nakamoto T, Ozaki T, Sugita K, Mizuno M, Araki H. Microstructural formation and characterization mechanisms of selective laser melted Al-Si-Mg alloys with increasing magnesium content. *Mater Sci Eng A* 2019;754:786-98. DOI

4. Kimura T, Nakamoto T, Mizuno M, Araki H. Effect of silicon content on densification, mechanical and thermal properties of Al-xSi binary alloys fabricated using selective laser melting. *Mater Sci Eng A* 2017;682:593-602. DOI

5. Suryawanshi J, Prashanth K, Scudino S, Eckert J, Prakash O, Ramamurty U. Simultaneous enhancements of strength and toughness in an Al-12Si alloy synthesized using selective laser melting. *Acta Mater* 2016;115:285-94. DOI

6. Wang P, Lao C, Chen Z, et al. Microstructure and mechanical properties of Al-12Si and Al-3.5Cu-1.5Mg-1Si bimetal fabricated by selective laser melting. *J Mater Sci Technol* 2020;36:18-26. DOI

7. Awd M, Siddique S, Walther F. Microstructural damage and fracture mechanisms of selective laser melted Al-Si alloys under fatigue loading. *Theor Appl Fract Mech* 2020;106:102483. DOI

8. Cerri E, Ghio E, Bolelli G. Effect of the distance from build platform and post-heat treatment of AlSi10Mg alloy manufactured by single- and multi-laser selective laser melting. *J Mater Eng Perform* 2021;30:4981-92. DOI

9. Chen B, Moon S, Yao X, et al. Strength and strain hardening of a selective laser melted AlSi10Mg alloy. *Scr Mater* 2017;141:45-9. DOI

10. Larrosa N, Wang W, Read N, et al. Linking microstructure and processing defects to mechanical properties of selectively laser melted AlSi10Mg alloy. *Theor Appl Fract Mech* 2018;98:123-33. DOI

11. Hwang WJ, Bang GB, Choa S. Effect of a stress relief heat treatment of AlSi7Mg and AlSi10Mg alloys on mechanical and electrical properties according to silicon precipitation. *Met Mater Int* 2022. DOI

12. Denti L. Additive manufactured A357.0 samples using the laser powder bed fusion technique: shear and tensile performance. *Metals* 2018;8:670. DOI

13. Yang KV, Rometsch P, Davies C, Huang A, Wu X. Effect of heat treatment on the microstructure and anisotropy in mechanical properties of A357 alloy produced by selective laser melting. *Mater Des* 2018;154:275-90. DOI

14. Suzuki A, Miyasaka T, Takata N, Kobashi M, Kato M. Control of microstructural characteristics and mechanical properties of AlSi12 alloy by processing conditions of laser powder bed fusion. *Addit Manuf* 2021;48:102383. DOI

15. Gheysen J, Marteleur M, van der Rest C, Simar A. Efficient optimization methodology for laser powder bed fusion parameters to manufacture dense and mechanically sound parts validated on AlSi12 alloy. *Mater Des* 2021;199:109433. DOI

16. Mei J, Han Y, Zu G, et al. Achieving superior strength and ductility of AlSi10Mg alloy fabricated by selective laser melting with large laser power and high scanning speed. *Acta Metall Sin* 2022;35:1665-72. DOI

17. Dai D, Gu D, Zhang H, et al. Influence of scan strategy and molten pool configuration on microstructures and tensile properties of selective laser melting additive manufactured aluminum based parts. *Opt Laser Technol* 2018;99:91-100. DOI

18. Giovagnoli M, Silvi G, Merlin M, Di Giovanni MT. Optimisation of process parameters for an additively manufactured AlSi10Mg alloy: limitations of the energy density-based approach on porosity and mechanical properties estimation. *Mater Sci Eng A* 2021;802:140613. DOI

19. Salandari-rabori A, Wang P, Dong Q, Fallah V. Enhancing as-built microstructural integrity and tensile properties in laser powder bed fusion of AlSi10Mg alloy using a comprehensive parameter optimization procedure. *Mater Sci Eng A* 2021;805:140620. DOI

20. Wang C, Zhu J, Wang G, et al. Effect of building orientation and heat treatment on the anisotropic tensile properties of AlSi10Mg fabricated by selective laser melting. *J Alloys Compd* 2022;895:162665. DOI

21. Li X, Yi D, Wu X, et al. Effect of construction angles on microstructure and mechanical properties of AlSi10Mg alloy fabricated by selective laser melting. *J Alloys Compd* 2021;881:160459. DOI

22. Maconachie T, Leary M, Zhang J, et al. Effect of build orientation on the quasi-static and dynamic response of SLM AlSi10Mg. *Mater Sci Eng A* 2020;788:139445. DOI

23. Gupta MK, Singla AK, Ji H, et al. Impact of layer rotation on micro-structure, grain size, surface integrity and mechanical behaviour of SLM Al-Si-10Mg alloy. *J Mater Res Technol* 2020;9:9506-22. DOI

24. Yadav P, Rigo O, Arvieu C, Lacoste E. Microstructural and mechanical aspects of AlSi7Mg0.6 alloy related to scanning strategies in L-PBF. *Int J Adv Manuf Technol* 2022;120:6205-23. DOI

25. Lu Z, Zhang L. Thermodynamic description of the quaternary Al-Si-Mg-Sc system and its application to the design of novel Sc-additional A356 alloys. *Mater Des* 2017;116:427-37. DOI

26. Lu Z, Zhang L, Wang J, Yao Q, Rao G, Zhou H. Understanding of strengthening and toughening mechanisms for Sc-modified Al-Si-(Mg) series casting alloys designed by computational thermodynamics. *J Alloys Compd* 2019;805:415-25. DOI

27. Liu G, Gao J, Che C, Lu Z, Yi W, Zhang L. Optimization of casting means and heat treatment routines for improving mechanical and corrosion resistance properties of A356-0.54Sc casting alloy. *Mater Today Commun* 2020;24:101227. DOI

28. Gao J, Li Z. Current situation and prospect of computationally assisted design in high-performance additive manufactured aluminum alloys: a review. *Acta Met Sin* 2022;59:87-105. DOI

29. Yi W, Liu G, Lu Z, Gao J, Zhang L. Efficient alloy design of Sr-modified A356 alloys driven by computational thermodynamics and

machine learning. *J Mater Sci Technol* 2022;112:277-90. DOI

30.   Gao J, Zhong J, Liu G, et al. A machine learning accelerated distributed task management system (Malac-Distmas) and its application in high-throughput CALPHAD computation aiming at efficient alloy design. *Adv Powder Mater* 2022;1:100005. DOI

31.   Wei M, Tang Y, Zhang L, Sun W, Du Y. Phase-field simulation of microstructure evolution in industrial A2214 alloy during solidification. *Metall and Mat Trans A* 2015;46:3182-91. DOI

32.   Gao J, Malchère A, Yang S, et al. Dewetting of Ni silicide thin film on Si substrate: in-situ experimental study and phase-field modeling. *Acta Mater* 2022;223:117491. DOI

33.   Yang S, Zhong J, Wang J, Gao J, Li Q, Zhang L. A novel computational model for isotropic interfacial energies in multicomponent alloys and its coupling with phase-field model with finite interface dissipation. *J Mater Sci Technol* 2023;133:111-22. DOI

34.   Zhang J, Yuan W, Song B, et al. Towards understanding metallurgical defect formation of selective laser melted wrought aluminum alloys. *Adv Powder Mater* 2022;1:100035. DOI

35.   Yi W, Liu G, Gao J, Zhang L. Boosting for concept design of casting aluminum alloys driven by combining computational thermodynamics and machine learning techniques. *J Mater Inf* 2021;1:11. DOI

36.   Zhang S, Yi W, Zhong J, Gao J, Lu Z, Zhang L. Computer alloy design of Ti modified Al-Si-Mg-Sr casting alloys for achieving simultaneous enhancement in strength and ductility. *Materials* 2022;16:306. DOI PubMed PMC

37.   Mondal B, Mukherjee T, Debroy T. Crack free metal printing using physics informed machine learning. *Acta Mater* 2022;226:117612. DOI

38.   Yu T, Mo X, Chen M, Yao C. Machine-learning-assisted microstructure-property linkages of carbon nanotube-reinforced aluminum matrix nanocomposites produced by laser powder bed fusion. *Nanotechnol Rev* 2021;10:1410-24. DOI

39.   He P, Liu Q, Kruzic JJ, Li X. Machine-learning assisted additive manufacturing of a TiCN reinforced AlSi10Mg composite with tailorable mechanical properties. *Mater Lett* 2022;307:131018. DOI

40.   Prashanth K, Scudino S, Klauss H, et al. Microstructure and mechanical properties of Al-12Si produced by selective laser melting: Effect of heat treatment. *Mater Sci Eng A* 2014;590:153-60. DOI

41.   Prashanth K, Scudino S, Eckert J. Tensile properties of Al-12Si fabricated via selective laser melting (SLM) at different temperatures. *Technologies* 2016;4:38. DOI

42.   Li X, Wang X, Saunders M, et al. A selective laser melting and solution heat treatment refined Al-12Si alloy with a controllable ultrafine eutectic microstructure and 25% tensile ductility. *Acta Mater* 2015;95:74-82. DOI

43.   Prashanth K, Scudino S, Eckert J. Defining the tensile properties of Al-12Si parts produced by selective laser melting. *Acta Mater* 2017;126:25-35. DOI

44.   Liu M, Wada T, Suzuki A, Takata N, Kobashi M, Kato M. Effect of annealing on anisotropic tensile properties of Al-12%Si alloy fabricated by laser powder bed fusion. *Crystals* 2020;10:1007. DOI

45.   Wang X, Zhang L, Fang M, Sercombe T. The effect of atmosphere on the structure and properties of a selective laser melted Al-12Si alloy. *Mater Sci Eng A* 2014;597:370-5. DOI

46.   Rashid R, Masood S, Ruan D, et al. Effect of energy per layer on the anisotropy of selective laser melted AlSi12 aluminium alloy. *Addit Manuf* 2018;22:426-39. DOI

47.   Zhang S, Ma P, Jia Y, et al. Microstructure and mechanical properties of Al-(12-20)Si Bi-material fabricated by selective laser melting. *Materials* 2019;12:2126. DOI PubMed PMC

48.   Siddique S, Imran M, Wycisk E, Emmelmann C, Walther F. Influence of process-induced microstructure and imperfections on mechanical properties of AlSi12 processed by selective laser melting. *J Mater Process Technol* 2015;221:205-13. DOI

49.   Kimura T, Nakamoto T. Microstructures and mechanical properties of A356 (AlSi7Mg0.3) aluminum alloy fabricated by selective laser melting. *Mater Des* 2016;89:1294-301. DOI

50.   Rao H, Giet S, Yang K, Wu X, Davies CH. The influence of processing parameters on aluminium alloy A357 manufactured by selective laser melting. *Mater Des* 2016;109:334-46. DOI

51.   Rao JH, Zhang Y, Fang X, Chen Y, Wu X, Davies CH. The origins for tensile properties of selective laser melted aluminium alloy A357. *Addit Manuf* 2017;17:113-22. DOI

52.   Casati R, Vedani M. Aging response of an A357 Al alloy processed by selective laser melting. *Adv Eng Mater* 2019;21:1800406. DOI

53.   de Menezes JT, Castrodeza EM, Casati R. Effect of build orientation on fracture and tensile behavior of A357 Al alloy processed by selective laser melting. *Mater Sci Eng A* 2019;766:138392. DOI

54.   Zou T, Ou Y, Zhu H, Li L. Effects of heat treatment on microstructure and tensile properties of AlSi7Mg alloy fabricated by selective laser melting. *Hot Work Technol* 2019;48:154-7. DOI

55.   Tang G, Feng T, Duan G, et al. Process and properties of AlSi7Mg alloy fabricated by laser selected melting. *Foundry Technol* 2020;41:219-22. DOI

56.   Zou T, Ou Y, Zhu H, Qin J. Microstructure and mechanical properties of selective laser melted AlSi7Mg alloy. Available from: http://www.mater-rep.com/EN/abstract/abstract2647.shtml [Last accessed on 28 Mar 2023].

57.   Cerri E, Ghio E. Aging profiles of AlSi7Mg0.6 and AlSi10Mg0.3 Alloys manufactured via laser-powder bed fusion: direct aging versus T6. *Materials* 2022;15:6126. DOI PubMed PMC

58.   Cacace S, Gökhan Demir A, Sala G, Mattia Grande A. Influence of production batch related parameters on static and fatigue resistance of LPBF produced AlSi7Mg0.6. *Int J Fatigue* 2022;165:107227. DOI

59.   Rao JH, Zhang Y, Zhang K, Wu X, Huang A. Selective laser melted Al-7Si-0.6Mg alloy with in-situ precipitation via platform heating

for residual strain removal. *Mater Des* 2019;182:108005. DOI

60. Lorusso M, Trevisan F, Calignano F, Lombardi M, Manfredi D. A357 alloy by LPBF for industry applications. *Materials* 2020;13:1488. DOI PubMed PMC

61. Read N, Wang W, Essa K, Attallah MM. Selective laser melting of AlSi10Mg alloy: Process optimisation and mechanical properties development. *Mater Des* 2015;65:417-24. DOI

62. Bagherifard S, Beretta N, Monti S, Riccio M, Bandini M, Guagliano M. On the fatigue strength enhancement of additive manufactured AlSi10Mg parts by mechanical and thermal post-processing. *Mater Des* 2018;145:28-41. DOI

63. Li W, Li S, Liu J, et al. Effect of heat treatment on AlSi10Mg alloy fabricated by selective laser melting: microstructure evolution, mechanical properties and fracture mechanism. *Mater Sci Eng A* 2016;663:116-25. DOI

64. Tradowsky U, White J, Ward R, Read N, Reimers W, Attallah M. Selective laser melting of AlSi10Mg: influence of post-processing on the microstructural and tensile properties development. *Mater Des* 2016;105:212-22. DOI

65. Hitzler L, Janousch C, Schanz J, et al. Direction and location dependency of selective laser melted AlSi10Mg specimens. *J Mater Process Technol* 2017;243:48-61. DOI

66. Casati R, Hamidi Nasab M, Coduri M, Tirelli V, Vedani M. Effects of platform pre-heating and thermal-treatment strategies on properties of AlSi10Mg alloy processed by selective laser melting. *Metals* 2018;8:954. DOI

67. Kan WH, Nadot Y, Foley M, Ridosz L, Proust G, Cairney JM. Factors that affect the properties of additively-manufactured AlSi10Mg: porosity versus microstructure. *Addit Manuf* 2019;29:100805. DOI

68. Xiong Z, Liu S, Li S, Shi Y, Yang Y, Misra R. Role of melt pool boundary condition in determining the mechanical properties of selective laser melting AlSi10Mg alloy. *Mater Sci Eng A* 2019;740-741:148-56. DOI

69. Padovano E, Badini C, Pantarelli A, Gili F, D'aiuto F. A comparative study of the effects of thermal treatments on AlSi10Mg produced by laser powder bed fusion. *J Alloys Compd* 2020;831:154822. DOI

70. Fiocchi J, Biffi CA, Colombo C, Vergani LM, Tuissi A. Ad hoc heat treatments for selective laser melted Alsi10mg alloy aimed at stress-relieving and enhancing mechanical performances. *JOM* 2020;72:1118-27. DOI

71. Li Z, Li Z, Tan Z, Xiong D, Guo Q. Stress relaxation and the cellular structure-dependence of plastic deformation in additively manufactured AlSi10Mg alloys. *Int J Plast* 2020;127:102640. DOI

72. Sert E, Hitzler L, Hafenstein S, Merkel M, Werner E, Öchsner A. Tensile and compressive behaviour of additively manufactured AlSi10Mg samples. *Prog Addit Manuf* 2020;5:305-13. DOI

73. Park T, Baek M, Hyer H, Sohn Y, Lee K. Effect of direct aging on the microstructure and tensile properties of AlSi10Mg alloy manufactured by selective laser melting process. *Mater Charact* 2021;176:111113. DOI

74. Ou Y, Zhang Q, Wei Y, et al. Evolution of heterogeneous microstructure and its effects on tensile properties of selective laser melted AlSi10Mg alloy. *J Mater Eng Perform* 2021;30:4341-55. DOI

75. Paul MJ, Liu Q, Best JP, et al. Fracture resistance of AlSi10Mg fabricated by laser powder bed fusion. *Acta Mater* 2021;211:116869. DOI

76. Riener K, Oswald S, Winkler M, Leichtfried GJ. Influence of storage conditions and reconditioning of AlSi10Mg powder on the quality of parts produced by laser powder bed fusion (LPBF). *Addit Manuf* 2021;39:101896. DOI

77. Chen S, Tan Q, Gao W, et al. Effect of heat treatment on the anisotropy in mechanical properties of selective laser melted AlSi10Mg. *Mater Sci Eng A* 2022;858:144130. DOI

78. Bisht MS, Gaur V, Singh I. On mechanical properties of SLM Al-Si alloy: Role of heat treatment-induced evolution of silicon morphology. *Mater Sci Eng A* 2022;858:144157. DOI

79. Van Cauwenbergh P, Samaee V, Thijs L, et al. Unravelling the multi-scale structure-property relationship of laser powder bed fusion processed and heat-treated AlSi10Mg. *Sci Rep* 2021;11:6423. DOI PubMed PMC

80. Thijs L, Kempen K, Kruth J, Van Humbeeck J. Fine-structured aluminium products with controllable texture by selective laser melting of pre-alloyed AlSi10Mg powder. *Acta Mater* 2013;61:1809-19. DOI

81. Kumar MS, Javidrad HR, Shanmugam R, Ramoni M, Adediran AA, Pruncu CI. Impact of print orientation on morphological and mechanical properties of L-PBF based AlSi7Mg parts for aerospace applications. *Silicon* 2022;14:7083-97. DOI

82. Ashby M. Multi-objective optimization in material design and selection. *Acta Mater* 2000;48:359-69. DOI

83. Zhao L, Song L, Santos Macías JG, et al. Review on the correlation between microstructure and mechanical performance for laser powder bed fusion AlSi10Mg. *Addit Manuf* 2022;56:102914. DOI